

MICROCOPY RESOLUTION TEST CHART
NATIONAL BUREAU OF STANDARDS-1963-A

12

AMMRC TR 83-18

AD

AD A132505

CHARACTERIZATION OF CERAMIC VANE MATERIALS FOR SOKVA AND TURBOALTERNATOR

GEORGE D. QUINN, DONALD R. MESSIER,
and LISELOTTE J. SCHIOLER
CERAMICS RESEARCH DIVISION

April 1983

Approved for public release; distribution unlimited

DTIC
ELECTE
SEP 16 1983
S B

ARMY MATERIALS AND MECHANICS RESEARCH CENTER
Watertown, Massachusetts 02172

FILE COPY 88 09 13 089

The findings in this report are not to be construed as an official Department of the Army position, unless so designated by other authorized documents.

Mention of any trade names or manufacturers in this report shall not be construed as advertising nor as an official indorsement or approval of such products or companies by the United States Government.

DISPOSITION INSTRUCTIONS

Destroy this report when it is no longer needed.
Do not return it to the originator.

UNCLASSIFIED

SECURITY CLASSIFICATION OF THIS PAGE (When Data Entered)

REPORT DOCUMENTATION PAGE		READ INSTRUCTIONS BEFORE COMPLETING FORM
1. REPORT NUMBER AMMRC TR 83-18	2. GOVT ACCESSION NO. A132505	3. RECIPIENT'S CATALOG NUMBER
4. TITLE (and Subtitle) CHARACTERIZATION OF CERAMIC VANE MATERIALS FOR 10KW TURBOALTERNATOR		5. TYPE OF REPORT & PERIOD COVERED Final
		6. PERFORMING ORG. REPORT NUMBER
7. AUTHOR(s) George D. Quinn Donald R. Messier Liselotte J. Schioler		8. CONTRACT OR GRANT NUMBER(s)
9. PERFORMING ORGANIZATION NAME AND ADDRESS Army Materials and Mechanics Research Center Watertown, Massachusetts 02172 DRXMR-MC		10. PROGRAM ELEMENT, PROJECT, TASK AREA & WORK UNIT NUMBERS D/A Project: 1L763702DG1105 AMCMS Code: 623702.G1100
11. CONTROLLING OFFICE NAME AND ADDRESS U.S. Army Materiel Development and Readiness Command, Alexandria, Virginia 22333		12. REPORT DATE
		13. NUMBER OF PAGES 25
14. MONITORING AGENCY NAME & ADDRESS (if different from Controlling Office)		15. SECURITY CLASS. (of this report) Unclassified
		15a. DECLASSIFICATION/DOWNGRADING SCHEDULE
16. DISTRIBUTION STATEMENT (of this Report) Approved for public release; distribution unlimited.		
17. DISTRIBUTION STATEMENT (of the abstract entered in Block 20, if different from Report)		
18. SUPPLEMENTARY NOTES		
19. KEY WORDS (Continue on reverse side if necessary and identify by block number) Silicon nitride Gas turbine engine Failure analysis Silicon carbide Mechanical properties Ceramics Fracture mechanics		
20. ABSTRACT (Continue on reverse side if necessary and identify by block number) <p style="text-align: center;">(SEE REVERSE SIDE)</p>		

UNCLASSIFIED

SECURITY CLASSIFICATION OF THIS PAGE(When Data Entered)

Block No. 20

ABSTRACT

Characterization was done on four vane candidate materials: hot-pressed silicon nitride, sintered silicon nitride, sintered silicon carbide, and siliconized silicon carbide, being considered for use in a small turbine engine. Chemistry, phase content, and room-temperature mechanical strength were in the ranges expected for such materials. Fracture locations and origins were identified whenever possible, and measurements of fracture mirror radii and flaw sizes were done to enable fracture mechanics parameters to be calculated. Oxidation resistance of all materials was excellent at 950 to 1100°C. High temperature (800 to 1200°C) mechanical behavior was characterized via stepped temperature stress rupture and conventional stress rupture testing. A possible instability was found in the sintered silicon nitride at 1000°C. The hot-pressed silicon nitride was subject to static fatigue at temperatures from 800 to 1100°C. The two silicon carbide materials performed adequately over the same temperature range.

UNCLASSIFIED

SECURITY CLASSIFICATION OF THIS PAGE(When Data Entered)

CONTENTS

	Page
INTRODUCTION.	1
ROOM-TEMPERATURE MECHANICAL PROPERTIES AND OXIDATION.	1
Introduction	1
Experimental Procedures.	1
Results and Discussion	3
HIGH-TEMPERATURE MECHANICAL TESTING	13
Introduction	13
Experimental Procedures.	13
Results and Discussion	14
SUMMARY	20
General Characterization	20
Room-temperature Mechanical Testing.	20
Fracture Mechanics Parameters.	21
Oxidation.	21
High-temperature Mechanical Testing.	21
CONCLUSIONS	22
ACKNOWLEDGEMENTS.	22
REFERENCES.	22

Accession		✓
EFT		
PI		
U		
J		
By		
Distribution		
Availability Codes		
Dist	Avail and/or	Special
A		



INTRODUCTION

The work described herein was part of the program "MM&T, High Temperature Turbine Nozzle for 10KW Power Unit." The program was sponsored by USAMERADCOM, Ft. Belvoir, Va., and the engine testing and development was done by Solar Turbines International, San Diego, Calif. AMMRC supported the program by providing consulting advice and by doing characterization of ceramic materials supplied by Solar.

An earlier study demonstrated the feasibility of improving component durability in a small gas turbine engine via use of ceramic materials.¹ Specifically, it was shown through rig and engine testing that hot erosion resistance was substantially improved by use of hot-pressed silicon nitride (HPSN) vane trailing edge inserts in the engine nozzle. The HPSN inserts, however, were produced by methods suitable only for one-of-a-kind items. The present program was therefore initiated to develop methods for low cost production of such ceramic components. Cost reduction is expected to result from the use of lower cost materials than HPSN and/or improved manufacturing methods.

Materials characterization is an important part of any such program. Characterization data are essential to the identification of potential critical materials problems and to define the minimum materials' properties needed to obtain acceptable engine performance. Such data are also essential for establishing specifications to be used in future procurement actions involving ceramic components.

ROOM-TEMPERATURE MECHANICAL PROPERTIES AND OXIDATION

Introduction

This part of the report gives various room-temperature (RT) characterization data as well as results of high-temperature (950 to 1100°C) oxidation tests on four vane insert candidate materials. These include hot pressed silicon nitride (HPSN), sintered silicon nitride (SSN), sintered silicon carbide (SSC), and siliconized silicon carbide (Si/SiC).

Experimental Procedures

1. Materials

The four materials investigated were selected from a number of potential material/process combinations.² The materials were supplied to AMMRC in the form of bend test specimens and actual vane inserts. Procurement requests specified that the bend specimens be fabricated, insofar as possible, in a fashion identical to that of the vane inserts, so that the properties of each would be comparable.*

* NAPIER, J.C. Personal Communication.

1. NAPIER, J. C., METCALFE, A. G., and DUFFY, T. E. *Application of Ceramic Nozzles to 10KW Engine*, Report No. S.O. 8-4376-7, Solar Turbines International, San Diego, Calif., 1979.
2. NAPIER, J. C., RUSSELL, A. D., and GULDEN, M. E. *Manufacturing Methods for Ceramic Nozzle Section of Gas Turbine Powered APU's*, Solar Turbines International, San Diego, Calif., U.S. Army Mobility Equipment Research and Development Center Interim Contract Report, Contract No. DAAK 70-78-C-0156, July, 1980.

The SSN was a commercial composition consisting of silicon nitride and a yttria sintering aid.* In this case specimens were received in two lots (denoted ACCI and ACCII). Each lot was formed with a different molding die. Vanes were formed by injection molding to shape, followed by sintering to high density. Vanes and bend specimens thus fabricated were used as-is without further machining. Some of the bend specimens were slightly warped, i.e., bowed along their long axes.

The HPSN was a standard commercial grade fabricated with the use of magnesia as a sintering aid.** The vanes were made by hot pressing a billet to partial net shape, cutting bars of approximate vane shape from the billet, slicing individual vanes from the bars, and final grinding to the finished shape. Edge and corner radii were created by a tumble grinding process.

The SSC was comprised of α -SiC powder and a proprietary sintering aid.† Vanes were made by slip casting and sintering. Bend specimens were cut from slabs made by the same process.

Si/SiC vanes were made by slip casting a SiC powder mix, followed by firing in the presence of silicon, to yield a material consisting of SiC grains bonded together by Si.†† The slip-cast green body was a bar having the vane contour shape, which after firing, was sliced to yield individual vanes.

2. General Characterization

Routine characterization procedures that were done included visual and low-power optical microscopic inspection, chemical analysis via emission and atomic absorption spectroscopy, x-ray diffraction analysis, and density measurement.

3. Mechanical Testing

The bend specimens were rectangular bars 51-mm long x 3.05-mm wide x 2.40-mm deep. Edges were either rounded to a typical radius of 0.25 mm or chamfered 0.13 mm. The specimens were tested at RT in four-point loading with inner and outer spans of 15.2 and 30.4 mm, respectively. The cross-head speed used was 0.05 mm/min. The specimens were long enough so that, on occasion, two breaks per specimen were possible. In such cases, care was taken to insure that the previously stressed portion of the specimen was not re-inserted into the inner gauge length.

4. Fractography

All fracture surfaces of bend specimens were carefully examined visually and by low-power optical microscopy. Scanning electron microscopy was also employed as required to examine those surfaces in greater detail. Of major interest was the identification of locations at which fracture initiated and of defects that initiated fracture. Photomicrographs and scanning electron photomicrographs were taken as needed. The fracture mirror radii were measured as the distance to the mirror-mist boundary, and are averages of measurements on macrographs and scanning electron

* An experimental vintage of SSN-800, 1979, Airsearch Casting Co., Torrance, Calif.

** Ceratloy 147A, Ceradyne Inc., Santa Ana, Calif.

† Sintered α -Silicon Carbide, 1980, Carborundum Co., Niagara Falls, N.Y.

†† NC-430 ("Crystal") Siliconized Silicon Carbide, Norton Co., Worcester, Mass.

micrographs. The flaws were assumed to be semicircular, and the sizes reported are the averages of measurements in several directions made on the scanning electron micrographs.

5. Oxidation

Oxidation tests were done on small specimens (100 mg) cut from bend bars. The specimens were placed on alumina chips in a platinum crucible and run in ambient air at various temperatures from 950 to 1100°C for times up to 76 hr. Weight change was recorded continuously as a function of time. As indicated below, however, weight changes were so slight as to be marginally detectable.

Results and Discussion

1. General Characterization

Our work was mainly done on bend specimens and only a cursory inspection was done on the ceramic vanes. Details of dimensional analysis (to determine whether dimensions were within tolerances) and surface finish measurements are given elsewhere.² SSC vanes were unavailable for inspection, but comments on vanes made from the other three materials follow.

The general appearance of the HPSN vanes was good. It was noted, however, that machining striations on their top and bottom surfaces ran in two directions. Some chips were seen on chamfered edges and deep grooves existed along the length of the chamfer in some instances. Miscellaneous surface scratches were evident, and "surface spots" suggested the presence of large grains or other inhomogeneities.

The sintered Si_3N_4 vanes had obvious surface flaws, including machining marks, pores, and metallic-looking deposits. Numerous molding marks were prominent, and pores were also noted on the chamfered edges of the vanes.

The Si/SiC vanes looked reasonably good. Numerous surface machining marks were seen, but all were parallel to the vane length and none were very deep. Pits of various sizes and miscellaneous scratches on the surface were present.

Results of chemical analyses of the vane materials are given in Table 1. The high contents of Al and Y in the SSN material stem from the use of Al_2O_3 and Y_2O_3 as sintering aids. Similarly, the HPSN has a significant content of Mg; MgO was the sintering aid for that material. The Fe and Al in the HPSN are probably impurities. The SSC is relatively pure except for its significant content of B, suggesting that a boron compound may have been used as a sintering aid. The Si/SiC contains impurities generally expected for this type of material.

Table 2 gives the results of determinations of major crystalline phases by means of x-ray diffraction analysis. As would be expected, the only major phase in the silicon nitride materials is $\beta\text{-Si}_3\text{N}_4$. The silicon carbide materials are mainly $\alpha\text{-SiC}$, with the Si/SiC material also containing Si.

2. Mechanical Testing Results

Table 3 summarizes the RT mechanical testing data that were obtained on bend specimens of the vane candidate materials. Also given in that table are density data. Fracture sources and locations are specified whenever possible. Identification of such features on the Si/SiC material was impossible.

Table 1. CHEMICAL ANALYSIS OF CERAMIC VANE MATERIALS

Values are all weight percent and obtained by emission spectroscopy except as noted

Element	ACC-I	ACC-II	CD	CA80	NC-430
Al	6.4*	6.4*	0.19	0.01-0.1	0.1-1.0
B	ND	ND	ND	0.5-1.0	~0.01
Ca	0.02*	0.02*	0.04*	0.01-0.1	~0.01
Co	ND	ND	ND	0.1-0.5	0.1-0.5
Cr	<0.03	<0.03	<0.03	ND	0.01-0.1
Cu	0.02	0.01	0.01	0.01-0.1	0.01-0.1
Fe	0.12	<0.06	0.30	0.01-0.1	0.1-1.0
Mg	0.003	0.002	0.67	0.01-0.1	0.01-0.1
Mn	<0.04	<0.04	<0.04	0.001-0.01	0.01-0.05
Mo	ND	ND	ND	ND	0.001-0.01
Ni	<0.05	<0.05	<0.05	~0.01	0.05-0.1
Ti	<0.02	<0.02	<0.04	0.01-0.1	0.01-0.1
V	ND	ND	ND	0.01-0.1	0.01-0.1
Y*	10.5	11.9	0.1	ND	ND
Zr	ND	ND	ND	ND	0.01-0.1

ND - Not determined

*Determined by atomic absorption

Table 2. RESULTS OF X-RAY DIFFRACTION ANALYSES OF CERAMIC VANE MATERIALS

Material	Major Phases
ACC I SSN	β -Si ₃ N ₄
ACC II SSN	β -Si ₃ N ₄
CD HPSN	β -Si ₃ N ₄
CA 80 SSC	α -SiC
NC-430 Si/SiC	α -SiC, Si

Table 4 gives the results of statistical analysis of the bend test data based on assumptions that the data conform to normal³ or Weibull⁴ distributions. The latter analysis was done using the maximum likelihood estimator (MLE) technique.⁵ For reasons to be discussed later, the SSN data from ACC I and ACC II batches were combined.

Figure 1 shows the four sets of fracture stress data plotted according to the Weibull distribution.⁴ The strength and Weibull modulus data reported here agree

3. STEEL, R. G. D., and TORRIE, J. H. *Principles and Procedures of Statistics*, McGraw-Hill, New York, 1960.
4. WEIBULL, W. A. *Statistical Distribution Function of Wide Applicability*, J. Appl. Mech., v. 18, 1951, pp. 293-297.
5. MASON, D., NEAL, D., and LENOE, E. *Statistical Data Evaluation Procedures*, MIL-H-DK-17, *Composite Materials for Aircraft and Aerospace Applications, Interim Report No. 1*, U.S. Army Materials and Mechanics Research Center, Engineering Standardization Division, December, 1980.

Table 3. ROOM TEMPERATURE MECHANICAL TEST DATA ON VANE CANDIDATE MATERIALS

Material	σ_f (MPa)	Source	Location	Material	σ_f (MPa)	Source	Location	Material	σ_f (MPa)	Source	Location	Material	σ_f (MPa)	Source	Location
I	361	P(2)	S		495	U	S		260	U	S		141	(4)	(4)
ACC	373	P(1)	I	CD	504	P/N(3)	S	CA80	278	U	S	NC-430	183		
Sintered Si_3N_4	375	P(1)	I	Hot-Pressed Si_3N_4	506	P/N(3)	I	Sintered SiC	290	N/P(3)	S	Siliconized SiC	187		
$\rho = 3,240$ kg/m ³	376	P(2)	S		509	P/N(3)	I		411	P/N(3)	S		190		
	405	P(2)	S		527	P/N(3)	S	$\rho = 3,190$ kg/m ³	422	N/P(3)	S		195	$\rho = 2,980$ kg/m ³	
	413	U(2)	S		539	U	C		434	P/N(3)	S		196		
	421	U(2)	S		539	P/N(3)	S		438	N/P(3)	I		199		
	426	P(2)	S		555	P/N(3)	C		459	N	I		200		
	443	U(2)	C		556	P/N(3)	S		506	P/N(3)	S		201		
	454	P(2)	S		561	P/N(3)	S		535	N/P(3)	I		206		
	458	P(2)	S		598	P/N(3)	S		540	N/P(3)	I		207		
	461	U(2)	S		600	P/N(3)	C/I		547	U	S		208		
	493	P(2)	S		604	U	S		611	U	S		210		
	497	P(2)	S		621	P/N(3)	I						215		
	516	P(2)	S		666	P/N(3)	I						218		
					723	U	C						229		
II	309	P(2)	S												
	333	P(1)	I												
	343	P(1)	I												
	362	P(1)	I												
	363	P(2)	S												
	423	P(1)	I												
	555	P(1)	I												

Key to symbols: C, corner; I, interior; N, material defect; P, pore; S, surface; U, unknown.

- (1) Large internal voids which appear to have resulted from laminations which opened up during sintering.
- (2) Pores much smaller than (1). Also appear to have resulted from processing.
- (3) Material defects are volume-distributed porosity.
- (4) Nature of fracture surface made identification of sources and locations impossible.

well with values obtained by Larsen⁶ in an independent study of the same materials. Such agreement is encouraging for design purposes; materials properties should be consistent and reproducible from batch to batch over extended periods of time.

3. Fractography

The major defects in the injection-molded SSN were pores that almost certainly stemmed from processing. In the first lot of material (ACC I in Table 3), these consisted of small surface pores such as are shown in Figure 2. In addition, many such pores contained metallic-looking inclusions. Although EDAX analysis of these inclusions showed the presence of (in descending order of quantity) Si, Ni, Fe, and

6. LARSEN, D. C. *Property Screening and Evaluation of Ceramic Turbine Engine Materials*, Air Force Materials Laboratory Contract Report No. AFML-TR-79-4188, IITRI, Chicago, Ill., 1979.

Table 4. STATISTICAL PARAMETERS OF FRACTURE ANALYSIS ON CERAMIC VANE MATERIALS

Distribution	Parameter	ACC	CD	CA80	NC-430
Normal	Number of Samples, n	22	16	13	16
	RMS Error	0.0437	0.0645	0.0664	0.0655
	Mean Fracture Stress (MPa)	416	569	441	199
	90% Confidence Limits	392-440	540-597	384-498	190-208
	Standard Deviation (MPa)	64	63	110	20
	90% Confidence Limits	52-88	51-94	87-174	16-29
Weibull (MLE Technique)	RMS Error	0.0442	0.0761	0.0604	0.0466
	Weibull Slope, m	6.6	8.0	4.4	12.8
	90% Confidence Limits	4.6-8.2	5.2-10.3	2.7-5.8	8.4-16.6
	Characteristic Value (MPa)	444	598	482	207
	90% Confidence Limits	418-472	563-636	426-546	199-215

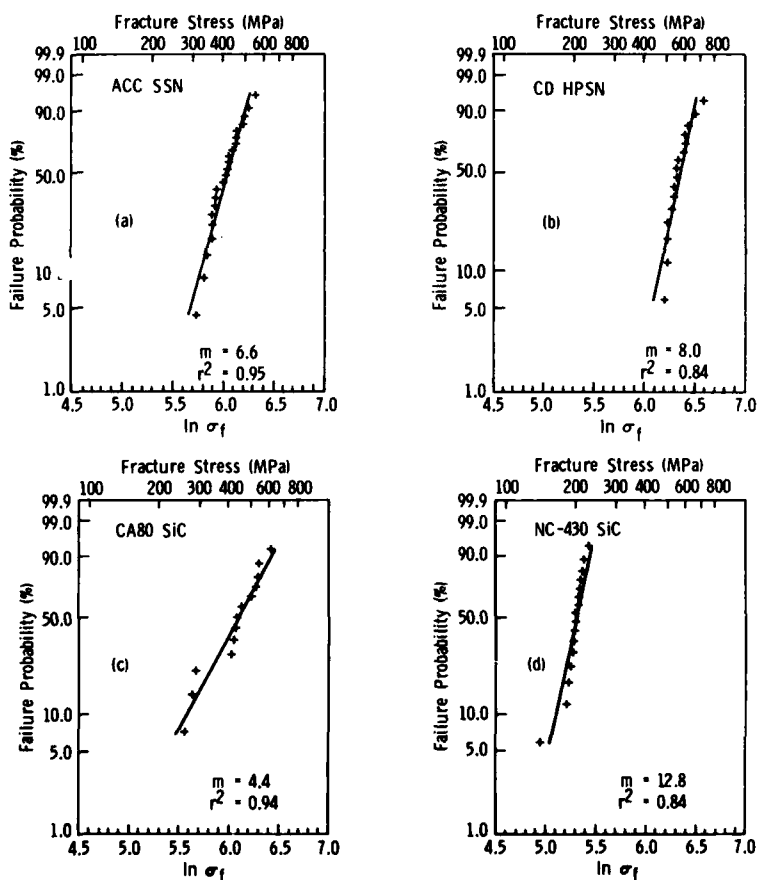


Figure 1. Ceramic vane materials bend test data plotted according to the Weibull distribution.

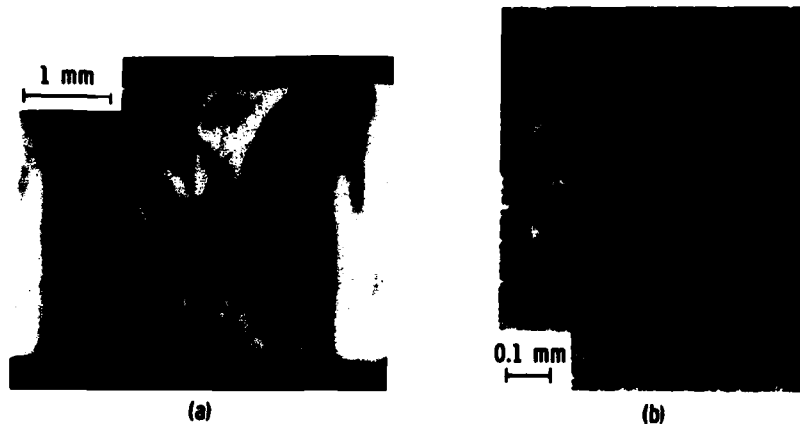


Figure 2. Failure from "small pore" defect in ACC sintered Si_3N_4 : (b) is a scanning electron photomicrograph of the right-hand part of the area encircled in (a).

Al, that technique cannot distinguish between the presence of Si in the form of Si_3N_4 or as a constituent in a metallic alloy. The shape and location of the surface pores suggests that they formed during the injection molding process.

The second lot of SSN (ACC II) contained defects consisting of large internal voids such as shown in Figure 3. It is likely that these also resulted from processing, probably from laminations that occurred during injection molding. The voids in the second lot were approximately five times as large as the surface pores in the first lot. Despite this, the difference between the average strengths of the two lots is statistically insignificant; a single tailed t-test⁴ showed that the difference is significant only at a low level (90 to 95%). The reason for this is apparently that large voids exist within the interiors of the bend specimens, whereas fractures initiate at surfaces where the tensile stress is highest. If the testing had been done in pure tension, the specimens with the large voids would surely have had lower strengths than the others.

As shown in Figure 4, the predominant type of flaw observed in the HPSN was a material defect consisting of porosity that was associated with abnormally large grains. These defects appeared as white spots on specimen surfaces. Although it seems reasonable to assume that such regions would result from inhomogeneous distribution of the MgO sintering aid, EDAX showed no detectable Mg in them. At present, therefore, no explanation can be given for their presence.

Porosity also was the most common flaw in the SSC material. Figure 5 shows an example of a specimen that failed from such a defect.

As already mentioned, and illustrated in Figure 6, the fracture surfaces of the Si/SiC material showed no features clearly identifiable as fracture origins. Locations where fracture initiated and defects that caused fracture could therefore not be determined.

Measurements of flaw sizes and fracture mirror radii were used to calculate several fracture mechanics parameters of interest. The results of the analysis follow.

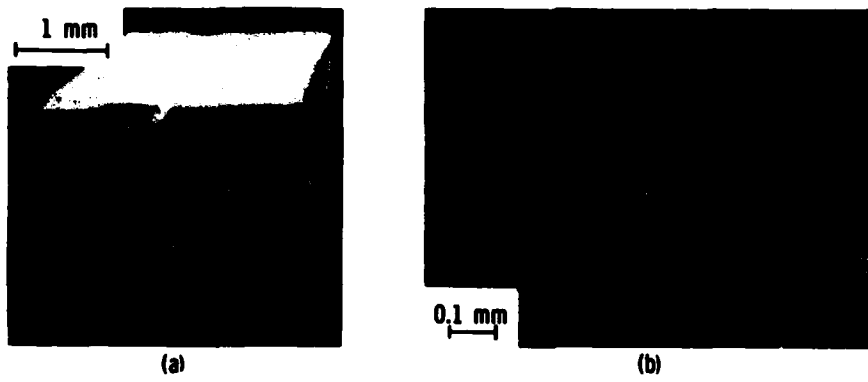


Figure 3. Two examples of "large pore" defects in ACC sintered Si_3N_4 .

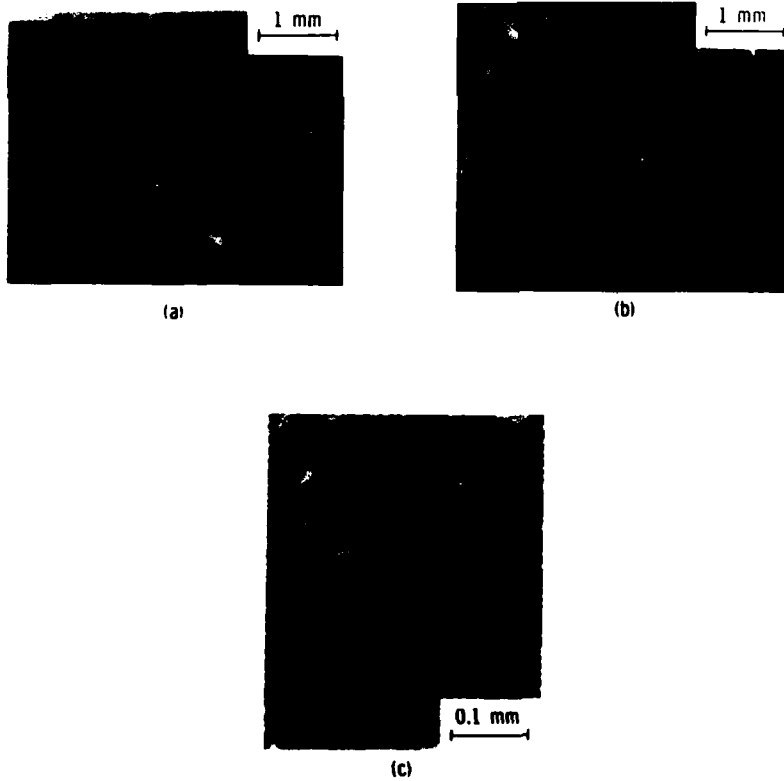


Figure 4. Failure from volume distributed porosity in CD hot-pressed Si_3N_4 : (a) surface appearance, (c) is a scanning electron photomicrograph of the right-hand part of the area encircled in (b).

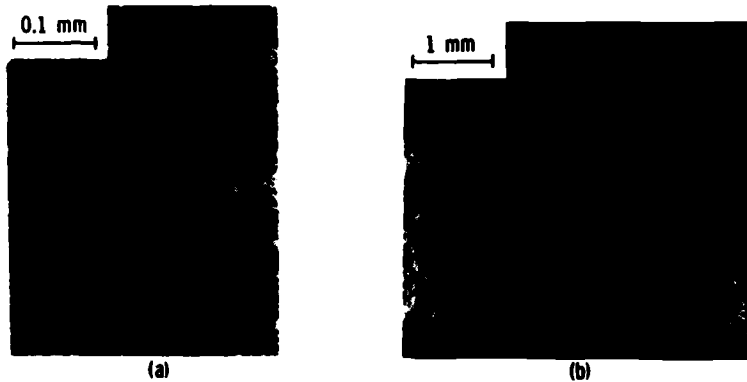


Figure 5. Failure from volume distributed porosity in CA80 sintered SiC: (a) is a scanning electron photomicrograph near the fracture origin of the surface shown in the left-hand part of the area encircled in (b). The area indicated by the arrow is the same in both pictures.

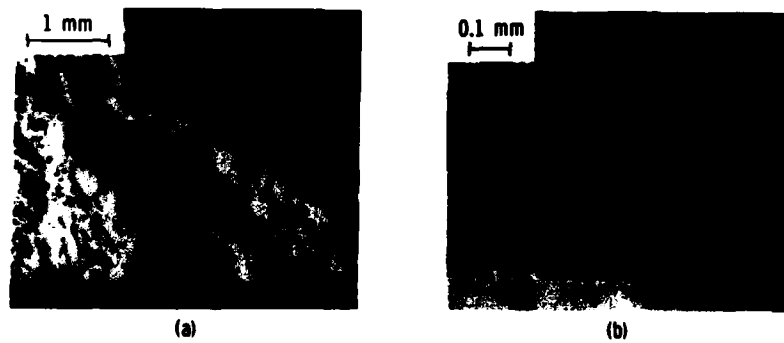


Figure 6. Fracture surfaces of NC-430 siliconized SiC bend specimen: (a) shows the generally featureless appearance of the surface. A few pores are visible in (b).

The critical stress intensity factor, K_{Ic} , is a measure of the resistance of a material to brittle fracture.⁷ This factor is related to the fracture stress, σ_f , and flaw size, c , as follows:

$$K_{Ic} = Y\sigma_f c^{1/2} ,$$

7. LAWN, B. R., and WILSHAW, T. R. *Fracture of Brittle Solids*, Cambridge University Press, Cambridge, U.K., 1975.

where Y is a geometric constant related to the flaw shape and loading mode. For the case of a shallow, semicircular surface crack in a beam in bending, Y will vary along the crack periphery, ranging in value from $Y = 1.35$ at the surface to $Y = 1.16$ at the deepest interior point.⁸ The choice of a value of Y to use in calculating K_{Ic} must allow for the fact that our flaw size values are averages of measurements taken in several directions. In view of this, it was decided to use the mean value of $Y = 1.26$ in our calculations, as did Mecholsky, et al.^{9*}

Figure 7 is a plot of strength vs flaw size for the three materials for which flaw size could be measured. For each material, a least-squares line has been fitted according to Equation (1). Equation (1) indicates the slope of the line is K_{Ic}/Y . The values of K_{Ic} listed in Figure 7 were obtained from this slope with the assumption that all flaws were semicircular surface defects for which $Y = 1.26$. In truth, the flaws had a variety of shapes and the assumption of a semicircular shape is a crude approximation. Therefore the values of K_{Ic} are only approximations.

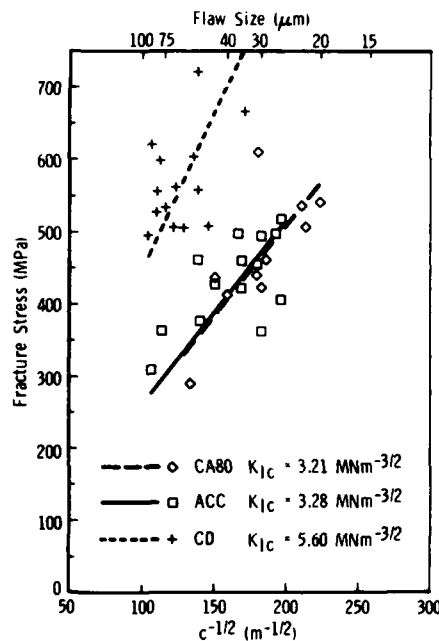


Figure 7. Strength vs flaw size for ceramic vane materials.

* It should be pointed out, however, that Mecholsky, et al.⁹ defined their geometric constant somewhat differently than we did.

8. SMITH, F. W., EMERY, A. F., and KOBAYASHI, A. S. *Stress Intensity Factors for Semicircular Cracks*, Trans ASME, Series E, v. 89, 1967, pp. 953-959.
9. MECHOLSKY, J. J., FREIMAN, S. W., and RICE, R. W. *Fracture Surface Analysis of Ceramics*, J. Mater. Sci., v. 11, 1976, pp. 1310-1319.

The fracture stress, σ_f , is empirically related to the fracture mirror radius, r_m , by

$$\sigma_f = A r_m^{-1/2}, \quad (2)$$

where A is a constant for a given material.^{9,10} Figure 8 shows the data for the three materials on which mirror measurements were possible, plotted according to Equation (2). Also shown are values of A calculated from least-squares fits of the data.

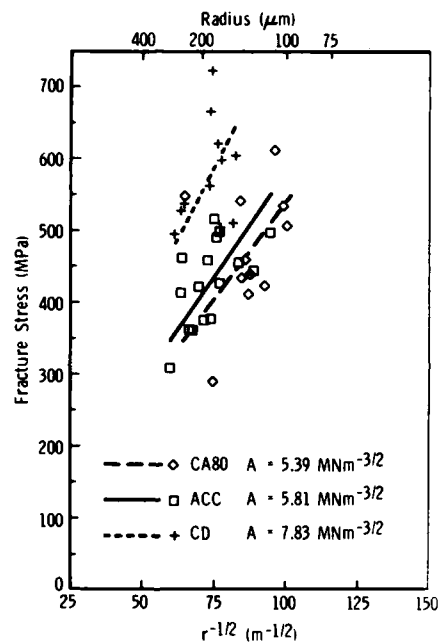


Figure 8. Strength vs fracture mirror radius for ceramic vane materials.

A relationship between the flaw size and fracture mirror radius may be obtained by combining Equations (1) and (2), i.e.,

$$K_{Ic} = YA (c/r_m)^{1/2}, \quad (3)$$

10. KIRCHNER, H. P., and KIRCHNER, J. W. *Fracture Mechanics of Fracture Mirrors*, J. Am. Ceram. Soc., v. 62 No. 3-4, 1979, pp. 198-202.

which shows that (c/r_m) should be constant for a given material and given flaw shape. Figure 9 shows plots of r_m vs c , as well as values of (r_m/c) obtained by least-squares analysis of the data. Two of the values thus obtained are approximately in the range of 4 to 8 reported to be common for polycrystalline ceramic materials,¹¹ while the value of 2.7 for HPSN is somewhat lower. In view of the difficulty of such measurements, as evidenced by the scatter in the data in Figure 9, such a discrepancy is not surprising.

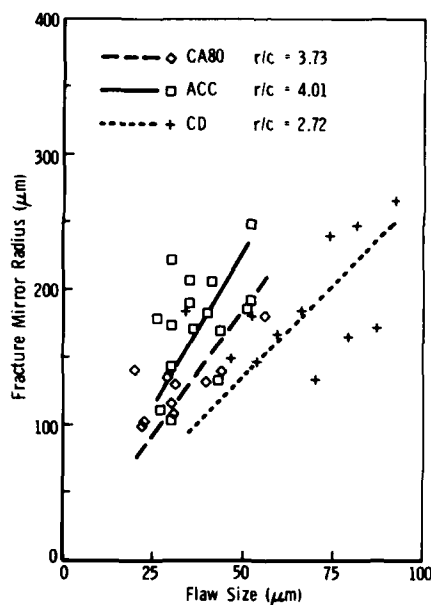


Figure 9. Fracture mirror radius vs flaw size for ceramic vane materials.

4. Oxidation Behavior

The data summarized in Table 5 were obtained to evaluate resistance of the vane candidate materials to oxidation over a temperature range similar to that in the engine. As shown in the table, oxidation weight gains over periods from 48 to 76 hr were negligible in all cases. The weight losses noted in a few instances are insignificant; the values given merely reflect the fact that changes were so slight as to be less than the precision of the measurement. No undesirable side reactions were noted, and it must be concluded that the oxidation resistance of all of the materials is adequate for the proposed application.

11. RICE, R. W. *The Difference in Mirror-to-Flaw Size Ratios Between Dense Glasses and Polycrystals*, J. Am. Ceram. Soc., v. 62 No. 9-10, 1979, pp. 533-536.

Army Materials and Mechanics Research Center
Watertown, Massachusetts 02172
CHARACTERIZATION OF CERAMIC VANE
MATERIALS FOR 10KW TURBOALTERNATOR
G. D. Quinn
D. R. Messler
L. J. Schioler

Technical Report AMMRC TR 83-18, May 1983, 25 pp-
illus-tables D/A Project: 1L763702D61105
AMCMS Code: 623702.61100

Characterization was done on four vane candidate materials, hot-pressed silicon nitride, sintered silicon nitride, sintered silicon carbide, and siliconized silicon carbide, being considered for use in a small turbine engine. Chemistry, phase content, and room-temperature mechanical strength were in the ranges expected for such materials. Fracture locations and origins were identified whenever possible, and measurements of fracture mirror radii and flaw sizes were done to enable fracture mechanics parameters to be calculated. Oxidation resistance of all materials was excellent at 950 to 1100°C. High temperature (800-1200°C) mechanical behavior was characterized via stepped temperature stress rupture and conventional stress rupture testing. A possible instability was found in the sintered silicon nitride at 1000°C. The hot-pressed silicon nitride was subject to static fatigue at temperatures from 800 to 1100°C. The two silicon carbide materials performed adequately over the same temperature range.

AD
UNCLASSIFIED
UNLIMITED DISTRIBUTION

Key Words
Silicon nitride
Silicon carbide
Ceramics

Army Materials and Mechanics Research Center
Watertown, Massachusetts 02172
CHARACTERIZATION OF CERAMIC VANE
MATERIALS FOR 10KW TURBOALTERNATOR
G. D. Quinn
D. R. Messler
L. J. Schioler

Technical Report AMMRC TR 83-18, May 1983, 25 pp-
illus-tables D/A Project: 1L763702D61105
AMCMS Code: 623702.61100

Characterization was done on four vane candidate materials, hot-pressed silicon nitride, sintered silicon nitride, sintered silicon carbide, and siliconized silicon carbide, being considered for use in a small turbine engine. Chemistry, phase content, and room-temperature mechanical strength were in the ranges expected for such materials. Fracture locations and origins were identified whenever possible, and measurements of fracture mirror radii and flaw sizes were done to enable fracture mechanics parameters to be calculated. Oxidation resistance of all materials was excellent at 950 to 1100°C. High temperature (800-1200°C) mechanical behavior was characterized via stepped temperature stress rupture and conventional stress rupture testing. A possible instability was found in the sintered silicon nitride at 1000°C. The hot-pressed silicon nitride was subject to static fatigue at temperatures from 800 to 1100°C. The two silicon carbide materials performed adequately over the same temperature range.

AD
UNCLASSIFIED
UNLIMITED DISTRIBUTION

Key Words
Silicon nitride
Silicon carbide
Ceramics

Army Materials and Mechanics Research Center
Watertown, Massachusetts 02172
CHARACTERIZATION OF CERAMIC VANE
MATERIALS FOR 10KW TURBOALTERNATOR
G. D. Quinn
D. R. Messler
L. J. Schioler

Technical Report AMMRC TR 83-18, May 1983, 25 pp-
illus-tables D/A Project: 1L763702D61105
AMCMS Code: 623702.61100

Characterization was done on four vane candidate materials, hot-pressed silicon nitride, sintered silicon nitride, sintered silicon carbide, and siliconized silicon carbide, being considered for use in a small turbine engine. Chemistry, phase content, and room-temperature mechanical strength were in the ranges expected for such materials. Fracture locations and origins were identified whenever possible, and measurements of fracture mirror radii and flaw sizes were done to enable fracture mechanics parameters to be calculated. Oxidation resistance of all materials was excellent at 950 to 1100°C. High temperature (800-1200°C) mechanical behavior was characterized via stepped temperature stress rupture and conventional stress rupture testing. A possible instability was found in the sintered silicon nitride at 1000°C. The hot-pressed silicon nitride was subject to static fatigue at temperatures from 800 to 1100°C. The two silicon carbide materials performed adequately over the same temperature range.

AD
UNCLASSIFIED
UNLIMITED DISTRIBUTION

Key Words
Silicon nitride
Silicon carbide
Ceramics

Army Materials and Mechanics Research Center
Watertown, Massachusetts 02172
CHARACTERIZATION OF CERAMIC VANE
MATERIALS FOR 10KW TURBOALTERNATOR
G. D. Quinn
D. R. Messler
L. J. Schioler

Technical Report AMMRC TR 83-18, May 1983, 25 pp-
illus-tables D/A Project: 1L763702D61105
AMCMS Code: 623702.61100

Characterization was done on four vane candidate materials, hot-pressed silicon nitride, sintered silicon nitride, sintered silicon carbide, and siliconized silicon carbide, being considered for use in a small turbine engine. Chemistry, phase content, and room-temperature mechanical strength were in the ranges expected for such materials. Fracture locations and origins were identified whenever possible, and measurements of fracture mirror radii and flaw sizes were done to enable fracture mechanics parameters to be calculated. Oxidation resistance of all materials was excellent at 950 to 1100°C. High temperature (800-1200°C) mechanical behavior was characterized via stepped temperature stress rupture and conventional stress rupture testing. A possible instability was found in the sintered silicon nitride at 1000°C. The hot-pressed silicon nitride was subject to static fatigue at temperatures from 800 to 1100°C. The two silicon carbide materials performed adequately over the same temperature range.

AD
UNCLASSIFIED
UNLIMITED DISTRIBUTION

Key Words
Silicon nitride
Silicon carbide
Ceramics

Army Materials and Mechanics Research Center
Waterloo, Massachusetts 02172
CHARACTERIZATION OF CERAMIC VANE
MATERIALS FOR 10KW TURBOALTERNATOR
G. D. Quinn
D. R. Messler
L. J. Schioler
Technical Report AMMRC TR 83-18, May 1983, 25 pp-
111us-tables D/A Project: IL763702D61105
AMCMS Code: 623702.61100

AD _____
UNCLASSIFIED
UNLIMITED DISTRIBUTION
Key Words
Silicon nitride
Silicon carbide
Ceramics

Characterization was done on four vane candidate materials, hot-pressed silicon nitride, sintered silicon nitride, sintered silicon carbide, and sintered silicon carbide, being considered for use in a small turbine engine. Chemistry, phase content, and room-temperature mechanical strength were in the ranges expected for such materials. Fracture locations and origins were identified whenever possible, and measurements of fracture mirror radii and flaw sizes were done to enable fracture mechanics parameters to be calculated. Oxidation resistance of all materials was excellent at 950 to 1100°C. High temperature (800-1200°C) mechanical behavior was characterized via stepped temperature stress rupture and conventional stress rupture testing. A possible instability was found in the sintered silicon nitride at 1000°C. The hot-pressed silicon nitride was subject to static fatigue at temperatures from 800 to 1100°C. The two silicon carbide materials performed adequately over the same temperature range.

Army Materials and Mechanics Research Center
Waterloo, Massachusetts 02172
CHARACTERIZATION OF CERAMIC VANE
MATERIALS FOR 10KW TURBOALTERNATOR
G. D. Quinn
D. R. Messler
L. J. Schioler
Technical Report AMMRC TR 83-18, May 1983, 25 pp-
111us-tables D/A Project: IL763702D61105
AMCMS Code: 623702.61100

AD _____
UNCLASSIFIED
UNLIMITED DISTRIBUTION
Key Words
Silicon nitride
Silicon carbide
Ceramics

Characterization was done on four vane candidate materials, hot-pressed silicon nitride, sintered silicon nitride, sintered silicon carbide, and sintered silicon carbide, being considered for use in a small turbine engine. Chemistry, phase content, and room-temperature mechanical strength were in the ranges expected for such materials. Fracture locations and origins were identified whenever possible, and measurements of fracture mirror radii and flaw sizes were done to enable fracture mechanics parameters to be calculated. Oxidation resistance of all materials was excellent at 950 to 1100°C. High temperature (800-1200°C) mechanical behavior was characterized via stepped temperature stress rupture and conventional stress rupture testing. A possible instability was found in the sintered silicon nitride at 1000°C. The hot-pressed silicon nitride was subject to static fatigue at temperatures from 800 to 1100°C. The two silicon carbide materials performed adequately over the same temperature range.

Army Materials and Mechanics Research Center
Waterloo, Massachusetts 02172
CHARACTERIZATION OF CERAMIC VANE
MATERIALS FOR 10KW TURBOALTERNATOR
G. D. Quinn
D. R. Messler
L. J. Schioler
Technical Report AMMRC TR 83-18, May 1983, 25 pp-
111us-tables D/A Project: IL763702D61105
AMCMS Code: 623702.61100

AD _____
UNCLASSIFIED
UNLIMITED DISTRIBUTION
Key Words
Silicon nitride
Silicon carbide
Ceramics

Characterization was done on four vane candidate materials, hot-pressed silicon nitride, sintered silicon nitride, sintered silicon carbide, and sintered silicon carbide, being considered for use in a small turbine engine. Chemistry, phase content, and room-temperature mechanical strength were in the ranges expected for such materials. Fracture locations and origins were identified whenever possible, and measurements of fracture mirror radii and flaw sizes were done to enable fracture mechanics parameters to be calculated. Oxidation resistance of all materials was excellent at 950 to 1100°C. High temperature (800-1200°C) mechanical behavior was characterized via stepped temperature stress rupture and conventional stress rupture testing. A possible instability was found in the sintered silicon nitride at 1000°C. The hot-pressed silicon nitride was subject to static fatigue at temperatures from 800 to 1100°C. The two silicon carbide materials performed adequately over the same temperature range.

Army Materials and Mechanics Research Center
Waterloo, Massachusetts 02172
CHARACTERIZATION OF CERAMIC VANE
MATERIALS FOR 10KW TURBOALTERNATOR
G. D. Quinn
D. R. Messler
L. J. Schioler
Technical Report AMMRC TR 83-18, May 1983, 25 pp-
111us-tables D/A Project: IL763702D61105
AMCMS Code: 623702.61100

AD _____
UNCLASSIFIED
UNLIMITED DISTRIBUTION
Key Words
Silicon nitride
Silicon carbide
Ceramics

Characterization was done on four vane candidate materials, hot-pressed silicon nitride, sintered silicon nitride, sintered silicon carbide, and sintered silicon carbide, being considered for use in a small turbine engine. Chemistry, phase content, and room-temperature mechanical strength were in the ranges expected for such materials. Fracture locations and origins were identified whenever possible, and measurements of fracture mirror radii and flaw sizes were done to enable fracture mechanics parameters to be calculated. Oxidation resistance of all materials was excellent at 950 to 1100°C. High temperature (800-1200°C) mechanical behavior was characterized via stepped temperature stress rupture and conventional stress rupture testing. A possible instability was found in the sintered silicon nitride at 1000°C. The hot-pressed silicon nitride was subject to static fatigue at temperatures from 800 to 1100°C. The two silicon carbide materials performed adequately over the same temperature range.

Table 5. RESULTS OF OXIDATION TESTS IN AIR
ON CERAMIC VANE MATERIALS

Material	Temperature (°C)	Time (hr)	Weight Change (mg/cm ²)	Estimated Oxide Thickness (μm)	Remarks
ACC-I	950	48	-	-	*
ACC-I	1000	51.5	+0.295	1.3	
ACC-II	1000	49	+0.208	0.9	
ACC-II	1100	72	+0.121	0.5	
NC-430	950	48	-0.027	-	*
NC-430	1000	76	+0.077	0.3	
CD	1000	72	+0.281	1.2	
CD	1100	50	+0.039	0.2	
CA80	1000	72	-0.282	-	*
CA80	1100	70	-0.750	-	*

*Slight weight loss occurred

HIGH-TEMPERATURE MECHANICAL TESTING

Introduction

The high-temperature load carrying ability of the vane candidate materials was evaluated via the stepped temperature stress rupture (STSR) test.^{12,13} Although the temperature history of a STSR specimen is more complex than one tested in a conventional test, the advantage of STSR testing is that it quickly identifies any unusual temperature sensitivity with a minimum of effort. The purpose of this part of the work was to screen the high-temperature mechanical behavior of the vane candidate materials as well as possible, given the limited number of specimens that were available.

Experimental Procedures

The STSR cycle employed is illustrated in Figure 10. At the start of a test, a specimen was loaded into a furnace fitted with a four-point bend fixture with inner and outer spans of 19 and 38 mm, respectively (see References 14 and 15 for details). The furnace was then heated to 800°C in air whereupon a deadweight load was applied to the specimen. The same load remained on the sample for the entire testing sequence. The furnace was held at 800°C until the sample broke or 24 hr passed. In the latter event the furnace was heated to 900°C (which took a few

12. QUINN, G. D., and KATZ, R. N. *Stepped Temperature Stress Rupture Testing of Silicon Based Ceramics*, Army Materials and Mechanics Research Center, Watertown, Mass., Technical Report No. TR 80-28, May, 1980.
13. QUINN, G. D., and KATZ, R. N. *Stepped Temperature Stress Rupture Testing of Silicon Based Ceramics*, Am. Ceram. Soc. Bull. v. 57, No. 11, 1978, pp. 1067-1068.
14. QUINN, G. D. *Guide to the Construction of a Simple 1800°C Test Furnace*, Army Materials and Mechanics Research Center, Watertown, Mass., Technical Report No. TR 83-1, January 1983.
15. QUINN, G. D. *Characterization of Turbine Ceramics after Long-Term Environmental Exposure*, Army Materials and Mechanics Research Center, Watertown, Mass., Technical Report No. TR 80-15, April, 1980.

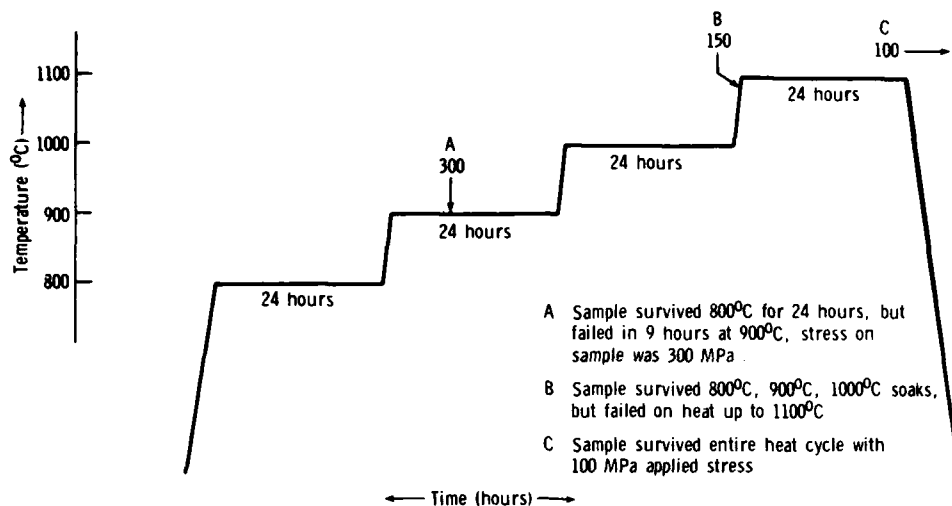


Figure 10. The STSR sequence employed in this study.

minutes) and again held for 24 hr. This procedure was repeated with additional 24-hr holds at 1000 and 1100°C. When a specimen broke, the furnace was cooled and unloaded. The time of failure was denoted by an arrow on the STSR plot. As detailed in the next section, a number of STSR tests were done at appropriate stress levels for each material. The load corresponding to a given stress level was calculated from the elastic beam formula.

In several instances, conventional stress rupture measurements were done to augment the STSR data. In such cases, the test procedure was the same except that the test temperature remained constant and the specimen was run as long as necessary (up to several hundred hours) for failure to occur.

Fracture surfaces of all specimens were examined visually and with a binocular microscope at magnifications to 100X. In cases in which creep occurred, creep strain was determined from the curvature of the inner gauge length of the flexural sample.

Results and Discussion

1. Sintered Silicon Nitride (SSN)

STSR trials were conducted with eight specimens from the first lot of SSN (ACC I), and two from the second lot (ACC II). As shown in Figure 11, three specimens failed upon loading, and seven others failed in a time dependent mode. Of the latter, one specimen failed after 0.4 hr at 800°C from a defect similar to those described in ROOM-TEMPERATURE MECHANICAL PROPERTIES AND OXIDATION, i.e., a pore containing a metallic deposit. No evidence of slow crack growth was seen on this particular specimen. On the other hand, zones of slow crack growth were clearly apparent on fracture surfaces of five of the six specimens that failed at or near 1000°C. The remaining specimen (from lot ACC II), was loaded at 100 MPa and lasted for 4.2 hr at 1000°C. It failed from a large internal void similar to

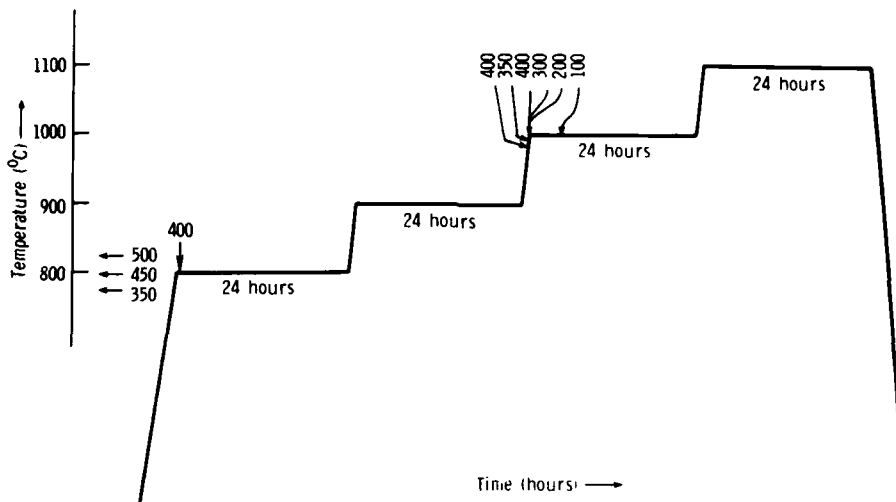


Figure 11 STSR results for ACC sintered silicon nitride.

those noted in ROOM-TEMPERATURE MECHANICAL PROPERTIES AND OXIDATION. The irregular nature of the surface of this defect apparently obscured any slow crack growth evidence that may have existed in this case. It should be noted that no creep deformation was observable in any of the specimens.

The STSR tests for SSN show that 1000°C is a critical temperature. Supplemental conventional stress rupture tests were conducted at 1100 and 1200°C . A sample loaded to 100 MPa survived 1300 hr at 1100°C with negligible creep deformation. Its retained strength was 383 MPa, a value similar to the RT reference strength. Another sample, loaded to 100 MPa at 1200°C survived 97 hr intact, whereupon the test was suspended due to excessive creep deformation ($> 1.5\%$ strain). Both samples survived much longer than similarly loaded samples at the critical temperature of 1000°C . This behavior may be related to other instabilities in yttria-containing silicon nitrides that have been reported previously.^{12,13,15,16-19}

2. Hot-Pressed Silicon Nitride (HPSN)

Figure 12 summarizes the results of STSR tests on HPSN. Of the 16 specimens tested, three failed immediately upon loading, two survived the entire sequence intact, and the remaining 11 failed in a time-dependent manner. The behavior of specimens that failed upon loading or shortly thereafter at 800°C suggests that fast fracture strength at that temperature is of the order of 400 MPa, a value

16. GAZZA, G. E., KNOCH, H., and QUINN, G. D. *Hot Pressed Si_3N_4 with Improved Thermal Stability*, Am. Ceram. Soc. Bull., v. 57, No. 11, 1978, pp. 1069-1080.
17. KNOCH, H., and GAZZA, G. E. *Effect of Carbon Impurity on the Thermal Degradation of a $\text{Si}_3\text{N}_4\text{-Y}_2\text{O}_3$ Ceramic*, J. Am. Ceram. Soc. v. 62, No. 11-12, 1979, pp. 634-636.
18. WEAVER, G. Q., and LUCEK, J. W. *Optimization of Hot Pressed $\text{Si}_3\text{N}_4\text{-Y}_2\text{O}_3$ Materials*, Am. Ceram. Soc. Bull., v. 57, No. 12, 1978, pp. 1131-1134, 1136.
19. LANGE, F. F., SINGHAL, S. C., and KUZNICKI, R. C. *Phase Relations and Stability Studies in the $\text{Si}_3\text{N}_4\text{-SiO}_2\text{-Y}_2\text{O}_3$ Pseudoternary System*, J. Am. Ceram. Soc. v. 60, No. 5-6, 1977, pp. 249-252.

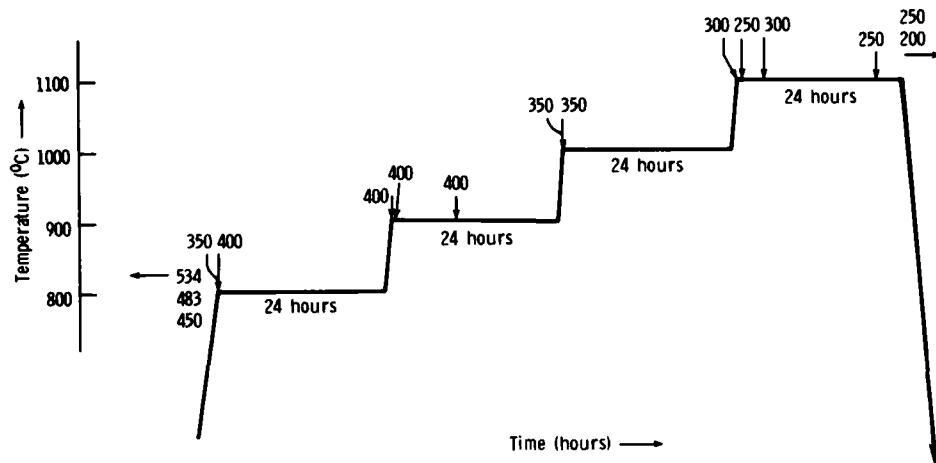


Figure 12. STSR results for CD hot-pressed silicon nitride.

significantly less than the average RT reference strength (569 MPa). Although time-dependent failures occurred over the entire temperature range of testing, there appeared to be no particular sensitivity to a given temperature. Stresses that caused delayed failure ranged from 250 to 400 MPa and the wide variations in times to failure observed for this material are similar to those observed previously for other ceramic materials.¹⁵

Fracture surfaces of the STSR specimens that failed at 800 to 1000°C resembled those of specimens that failed at RT. In all cases, well-defined fracture mirrors were evident. In contrast, evidence of slow crack growth was found on fracture surfaces of specimens that failed at 1100°C. Those latter specimens also had permanent creep deformation. Both surviving specimens had noticeable curvature with permanent tensile strains of 0.2%. Creep cracks were present that eventually would have grown to failure. RT retained strengths were 558 and 396 MPa for surviving specimens loaded at 200 and 250 MPa, respectively. The specimen loaded at 250 MPa showed evidence of slow crack growth while the other did not.

Although STSR testing indicated that slow crack growth contributed to failure at 1100°C, the failure mechanism at the lower temperatures was uncertain. Two conventional stress rupture tests were therefore done at 900°C to investigate this point further. A specimen loaded to 350 MPa failed after 307 hr at 900°C and subsequent examination revealed a small irregularity on the fracture mirror indicating that slow crack growth had occurred. The specimen showed no evidence of creep, however. A second specimen survived intact after 2000 hr at 300 MPa, and had only a small creep curvature ($\sim 0.05\%$ strain). The RT retained strength of that specimen was 711 MPa, a value substantially above the reference strength. A final test was done at 1100°C to determine whether a stress rupture limit may exist at that temperature. The specimen showed modest curvature (0.6% tensile strain) after surviving 2000 hr at 200 MPa, and its RT retained strength was 393 MPa, well below the reference strength. In this case, the fracture origin was identified as a large inclusion and there was no evidence of slow crack growth.

In summary, the STSR results showed the HPSN to be susceptible to static fatigue at all temperatures between 800 and 1100°C at stress levels from 250 to 400 MPa. The fast fracture strength of the material at 800°C is well below the RT reference strength. Slow crack growth occurs at 1100°C, and probably at lower temperatures as well, although fractographic evidence of such behavior is difficult to detect at the lower temperatures. Careful scanning electron microscopy would be useful in resolving this point. Creep deformation became significant at 1100°C.

3. Sintered Silicon Carbide (SSC)

Figure 13 shows the results of the 11 STSR tests that were done on SSC. Four specimens failed on loading, three failed in a time-dependent manner at 800°C, and four others survived the entire cycle. The fast fracture strength at 800°C for this material does not differ appreciable from the RT reference value of 441 MPa. The specimens that failed after reaching 800°C did so quickly; times to failure were 7, 158, and 220 sec for specimens loaded at 300, 450, and 400 MPa, respectively. A large processing crack caused failure in the specimen that failed most rapidly. Fracture origins were found via fracture mirrors in the other two specimens, but any critical defects that were present were too small to see by low-power optical microscopy. As shown in Figure 14, however, examination by scanning electron microscopy revealed that fracture in the specimen that failed after 220 sec initiated at a surface-connected pore.

Excellent creep resistance was indicated by the fact that the four surviving specimens had negligible deformation. Their retained strengths of 453, 465, 466, and 469 MPa were remarkably similar and comparable to the RT reference strength of 441 MPa.

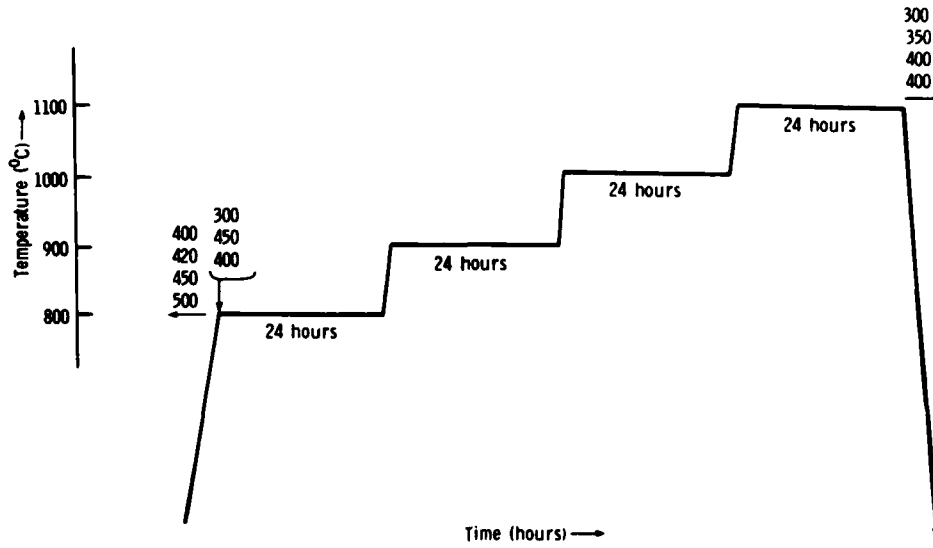


Figure 13. STSR results for CABO sintered silicon carbide.

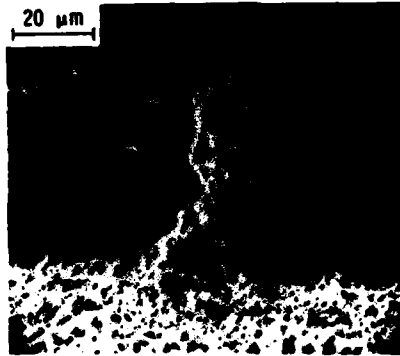


Figure 14. Carborundum sintered alpha silicon carbide sample that failed in the STSR sequence at 800°C.

The low scatter in the retained strength values after STSR testing indicated that further experiments should be done to see whether the effect was real and, if so, whether it was due to heat treatment alone or a combination of heat and stress. Therefore, four additional specimens were subjected to the STSR temperature sequence with no applied load. Their retained strengths were 215, 458, 477, and 519 MPa. The low strength specimen failed from an obvious processing crack, and that value should be ignored. While there is some difference in the scatter between specimens tested with and without stress at high temperature, there is insufficient data to draw any firm conclusions.

A series of conventional stress rupture tests at 1200°C was done on SSC to determine whether the present lot of material had properties similar to those reported previously for the same material.^{15,20,21} The results of the present testing appear in Table 6. There are insufficient data to present in graphical form, but the results are entirely consistent with those obtained previously.

In summary, SSC exhibits good resistance to creep deformation and static fatigue failure in the temperature range from 800 to 1100°C. As previously found,^{15,20,21} the most likely source of time dependent failure is surface-connected porosity, and such failures occur only at stresses greater than 70% of the fast fracture strength of the material.

20. QUINN, G.D., and KATZ, R.N. *Time Dependent High Temperature Strength of Sintered α -SiC*, J. Am. Ceram. Soc. v. 63, No. 1-2, 1980, pp. 117-119.
21. SRINIVASAN, M. *Elevated Temperature Stress Rupture Response of Sintered Alpha Silicon Carbide*, Presentation at 81st Annual Meeting of Am. Ceram. Soc., Cincinnati, Ohio, April 27, 1979, manuscript available from The Carborundum Company, Niagara Falls, N.Y.

Table 6. RESULTS OF STRESS RUPTURE TESTS ON SINTERED SILICON CARBIDE (CA 80) AT 1200°C

Applied Stress (MPa)	Time to Failure (hr)
500	Failed on Loading
500	Failed on Loading
400	Failed on Loading
400	0.04
400	13.7
400	138.3
400	321.3
400	399.2
300	28.9
300	112.8

4. Siliconized Silicon Carbide (Si/SiC)

The results of STSR tests done on this material are shown in Figure 15. Of the 12 specimens tested, five failed during loading, four survived intact, and three failed in a time-dependent manner. Specimens loaded to 200 MPa broke on loading while most loaded to 180 MPa did not, indicating that fast fracture strength at 800°C is only slightly below that at RT (199 MPa). The three specimens that failed in a time-dependent manner did so at low temperatures and failure origins could not be identified in any of them. The four surviving specimens had only slight permanent creep strains of the order of 0.05%. The RT retained strengths of the survivors were 229, 243, 245, and 259 MPa, which are all well above the reference strength. Such results suggest that flaw healing may have occurred during heat treatment. No correlation was apparent between retained strength and stress applied during STSR testing.

Four conventional stress-rupture tests were done to determine whether such failures would occur at 700°C. All specimens were loaded to 180 MPa, and results were mixed: two failed on loading, one broke after 52 hr, and the final one survived 2000 hr. The latter specimen had no creep deformation and its retained strength was 280 MPa.

The above results indicate that Si/SiC has good resistance to static fatigue failure and to creep deformation over the temperature range from 700 to 1100°C.

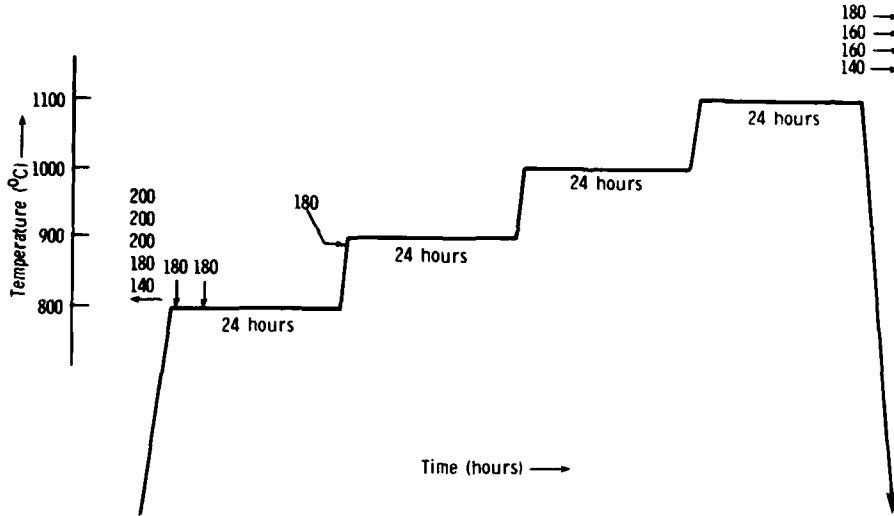


Figure 15. STSR results for NC430 silicon carbide.

SUMMARY

The results of characterization tests on four ceramic vane candidate materials: sintered silicon nitride (SSN), hot-pressed silicon nitride (HPSN), sintered silicon carbide (SSC), and siliconized silicon carbide (Si/SiC), may be summarized as follows:

General Characterization

Inspection of surfaces of vanes and bend bars showed them to be in acceptable condition. Chemical and x-ray analyses indicated that compositions were as expected for these materials.

Room-temperature Mechanical Testing

1. SSN

The average strength of this 416 ± 64 MPa; the principal defects observed were voids (gross in some cases), apparently from processing.

2. HPSN

Average strength was found to be 569 ± 63 MPa; defects were inclusions consisting of porosity associated with abnormally large grains.

3. SSC

The average strength of this material was 441 ± 110 MPa; defects were internal pores.

4. Si/SiC

The average strength was 199 ± 20 MPa; its relatively coarse microstructure made identification of critical defects impossible.

Fracture Mechanics Parameters

Values of the critical stress intensity factor, K_{Ic} were calculated for all of the materials except Si/SiC. All values appear reasonable. Ratios of fracture mirror radius to flaw size were slightly lower than expected.

Oxidation

All of the materials showed excellent resistance to oxidation in air at temperatures from 950 to 1100°C for times up to 76 hr.

High-temperature Mechanical Testing

1. SSN

This material showed a possible temperature-related instability at 1000°C. Creep was minimal from 800 to 1100°C. A number of failures resulted from gross voids related to processing.

2. HPSN

This material showed evidence of static fatigue over the entire temperature range of testing, 800 to 1100°C, at loads ranging from 250 to 400 MPa. Estimated safe stress limits are 300 MPa at 900°C and 200 MPa at 1100°C. Significant creep deformation occurred at 1100°C.

3. SSC

Sintered silicon carbide showed excellent resistance to creep and static fatigue from 800 to 1100°C. Fast fracture strength at 800°C was close to that at RT. Time-dependent failure occurred at stresses of 70% or more of the fast fracture value, suggesting that a safe stress level would be 300 MPa over the temperature range of 800 to 1100°C. Principal defects were surface-connected pores and, occasionally, cracks. Evidence suggests that heat treatment may reduce scatter in strength.

4. Si/SiC

This material had good resistance to creep and static fatigue from 800 to 1100°C, and it is estimated that it could be safely used at stresses of 150 MPa or less under these conditions. Microstructures of fracture surfaces were difficult to interpret, making identification of critical defects impossible.

CONCLUSIONS

The present work was performed to evaluate four candidate materials for use in a small, radial gas turbine. Chemistry, phase content, and room temperature mechanical strength were in the ranges expected for such materials. High-temperature stress rupture behavior was different for the four materials. The two silicon carbides were less prone to static fatigue failure than were the nitrides. It, nevertheless, remains to be demonstrated whether the properties measured on laboratory scale samples are representative of larger scale components or production quantities.

ACKNOWLEDGEMENTS

The authors appreciate the support of USAMERADCOM, Ft. Belvoir, Va., in making the work possible. In particular, the help of J.P. Arnold and W.F. McGovern is gratefully acknowledged. Also appreciated is the assistance of J.C. Napier and A.D. Russell of Solar Turbines International, San Diego, CA who supplied the specimens that were used. A.F. Connolly is acknowledged for providing excellent scanning electron micrographs.

REFERENCES

1. NAPIER, J. C., METCALFE, A. G., and DUFFY, T. E. *Application of Ceramic Nozzles to 10KW Engine*, Report No. S.O. 6-4375-7, Solar Turbines International, San Diego, Calif., 1979.
2. NAPIER, J. C., RUSSELL, A. D., and GULDEN, M. E. *Manufacturing Methods for Ceramic Nozzle Section of Gas Turbine Powered APU's*, Solar Turbines International, San Diego, Calif., U.S. Army Mobility Equipment Research and Development Center Interim Contract Report, Contract No. DAAK 70-78-C-0156, July, 1980.
3. STEEL, R. G. D., and TORRIE, J. H. *Principles and Procedures of Statistics*, McGraw-Hill, New York, 1960.
4. WEIBULL, W. A. *Statistical Distribution Function of Wide Applicability*, J. Appl. Mech., v. 18, 1951, pp. 293-297.
5. MASON, D., NEAL, D., and LENOE, E. *Statistical Data Evaluation Procedures*, MIL-H-DK-17, *Composite Materials for Aircraft and Aerospace Applications, Interim Report No. 1*, U.S. Army Materials and Mechanics Research Center, Engineering Standardization Division, December, 1980.
6. LARSEN, D. C. *Property Screening and Evaluation of Ceramic Turbine Engine Materials*, Air Force Materials Laboratory Contract Report No. AFML-TR-79-4188, IITRI, Chicago, Ill., 1979.
7. LAWN, B. R., and WILSHAW, T. R. *Fracture of Brittle Solids*, Cambridge University Press, Cambridge, U.K., 1975.
8. SMITH, F. W., EMERY, A. F., and KOBAYASHI, A. S. *Stress Intensity Factors for Semicircular Cracks*, Trans ASME, Series E, v. 89, 1967, pp. 963-969.
9. MECHOLSKY, J. J., FREIMAN, S. W., and RICE, R. W. *Fracture Surface Analysis of Ceramics*, J. Mater. Sci., v. 11, 1976, pp. 1310-1319.
10. KIRCHNER, H. P., and KIRCHNER, J. W. *Fracture Mechanics of Fracture Mirrors*, J. Am. Ceram. Soc., v. 62 No. 3-4, 1979, pp. 198-202.
11. RICE, R. W. *The Difference in Mirror-to-Flew Size Ratios Between Dense Glasses and Polycrystals*, J. Am. Ceram. Soc., v. 62 No. 9-10, 1979, pp. 533-535.
12. QUINN, G. D., and KATZ, R. N. *Stepped Temperature Stress Rupture Testing of Silicon Based Ceramics*, Army Materials and Mechanics Research Center, Watertown, Mass., Technical Report No. TR 80-28, May, 1980.
13. QUINN, G. D., and KATZ, R. N. *Stepped Temperature Stress Rupture Testing of Silicon Based Ceramics*, Am. Ceram. Soc. Bull., v. 57, No. 11, 1978, pp. 1057-1068.
14. QUINN, G. D. *Guide to the Construction of a Simple 1600°C Test Furnace*, Army Materials and Mechanics Research Center, Watertown, Mass., Technical Report No. TR 83-1, January, 1983.
15. QUINN, G. D. *Characterization of Turbine Ceramics after Long-Term Environmental Exposure*, Army Materials and Mechanics Research Center, Watertown, Mass., Technical Report No. TR 80-15, April, 1980.
16. GAZZA, G. E., KNOCH, H., and QUINN, G. D. *Hot Pressed Si_3N_4 with Improved Thermal Stability*, Am. Ceram. Soc. Bull., v. 57, No. 11, 1978, pp. 1059-1060.
17. KNOCH, H., and GAZZA, G. E. *Effect of Carbon Impurity on the Thermal Degradation of a $Si_3N_4-Y_2O_3$ Ceramic*, J. Am. Ceram. Soc., v. 62, No. 11-12, 1979, pp. 634-635.
18. WEAVER, G. Q., and LUCEK, J. W. *Optimization of Hot Pressed $Si_3N_4-Y_2O_3$ Materials*, Am. Ceram. Soc. Bull., v. 57, No. 12, 1978, pp. 1131-1134, 1136.
19. LANGE, F. F., SINGHAL, S. C., and KUZNICKI, R. C. *Phase Relations and Stability Studies in the $Si_3N_4-SiO_2-Y_2O_3$ Pseudoternary System*, J. Am. Ceram. Soc., v. 60, No. 5-6, 1977, pp. 249-252.
20. QUINN, G. D., and KATZ, R. N. *Time Dependent High Temperature Strength of Sintered α -SiC*, J. Am. Ceram. Soc., v. 63, No. 1-2, 1980, pp. 117-119.
21. SRINIVASAN, M. *Elevated Temperature Stress Rupture Response of Sintered Alpha Silicon Carbide*, Presentation at 81st Annual Meeting of Am. Ceram. Soc., Cincinnati, Ohio, April 27, 1979, manuscript available from The Carborundum Company, Niagara Falls, N.Y.

DISTRIBUTION LIST

No. of Copies	To	No. of Copies	To
1	Office of the Under Secretary of Defense for Research and Engineering, The Pentagon, Washington, DC 20310	1	Commander, U.S. Army Natick Research and Development Laboratories, Natick, MA 01760
1	ATTN: Mr. J. Persh	1	ATTN: Technical Library
1	Dr. G. Gamota	1	Dr. J. Hanson
12	Commander, Defense Technical Information Center, Cameron Station, Building 5, 5010 Duke Street, Alexandria, VA 22314	1	Commander, U.S. Army Satellite Communications Agency, Fort Monmouth, NJ 07703
1	National Technical Information Service, 5285 Port Royal Road, Springfield, VA 22161	1	ATTN: Technical Document Center
1	Director, Defense Advanced Research Projects Agency, 1400 Wilson Boulevard, Arlington, VA 22209	1	Commander, U.S. Army Tank-Automotive Command, Warren, MI 48090
1	ATTN: Dr. A. Bement	1	ATTN: Dr. W. Bryzik
1	Dr. Van Reuth	1	Mr. E. Hamperian
1	MAJ Harry Winsor	1	D. Rose
1	Battelle Columbus Laboratories, Metals and Ceramics Information Center, 505 King Avenue, Columbus, OH 43201	1	DRSTA-RKA
1	ATTN: Mr. Winston Duckworth	1	DRSTA-UL, Technical Library
1	Dr. D. Niesz	1	DRSTA-R
1	Dr. R. Wills	1	Commander, U.S. Army Armament Research and Development Command, Dover, NJ 07801
1	Deputy Chief of Staff, Research, Development, and Acquisition, Headquarters, Department of the Army, Washington, DC 20310	1	ATTN: Mr. J. Lannon
1	ATTN: DAMA-ARZ	1	Dr. G. Vezzoli
1	DAMA-CSS, Dr. J. Bryant	1	Mr. A. Graf
1	DAMA-PPP, Mr. R. Vawter	1	Mr. Harry E. Pebly, Jr., PLASTEC, Director
1	Commander, Army Research Office, P.O. Box 12211, Research Triangle Park, NC 27709	1	Technical Library
1	ATTN: Information Processing Office	1	Commander, U.S. Army Armament Materiel Readiness Command, Rock Island, IL 61299
1	Dr. G. Mayer	1	ATTN: Technical Library
1	Dr. J. Hurt	1	Commander, Aberdeen Proving Ground, MD 21005
1	Commander, U.S. Army Materiel Development and Readiness Command, 5001 Eisenhower Avenue, Alexandria, VA 22333	1	ATTN: DRDAR-CLB-PS, Mr. J. Vervier
1	ATTN: DRCDMD-ST	1	Commander, U.S. Army Mobility Equipment Research and Development Command, Fort Belvoir, VA 22060
1	DRCLDC	1	ATTN: DRDME-EM, Mr. W. McGovern
1	Commander, Harry Diamond Laboratories, 2800 Powder Mill Road, Adelphi, MD 20783	1	DRDME-V, Mr. E. York
1	ATTN: Mr. A. Benderly	1	DRDME-X, Mr. H. J. Peters
1	Technical Information Office	1	DRDME-, Mr. J. Napier
1	DELHD-RAE	1	Director, U.S. Army Ballistic Research Laboratory, Aberdeen Proving Ground, MD 21005
1	Commander, U.S. Army Missile Command, Redstone Arsenal, AL 35809	1	ATTN: DRDAR-TSB-S (STINFO)
1	ATTN: Mr. P. Ormsby	1	Commander, Rock Island Arsenal, Rock Island, IL 61299
1	Technical Library	1	ATTN: SARRI-EN
1	DRSMI-TB, Redstone Scientific Information Center	1	Commander, U.S. Army Test and Evaluation Command, Aberdeen Proving Ground, MD 21005
1	Commander, U.S. Army Aviation Research and Development Command, 4300 Goodfellow Boulevard, St. Louis, MO 63120	1	ATTN: DRSTE-ME
1	ATTN: DRDAV-EGX	1	Commander, U.S. Army Foreign Science and Technology Center, 220 7th Street, N.E., Charlottesville, VA 22901
1	DRDAV-QE	1	ATTN: Military Tech, Mr. W. Marley
1	Technical Library	1	Chief, Benet Weapons Laboratory, LCHSL, USA ARRADCOM, Watervliet, NY 12189
		1	ATTN: DRDAR-LCB-TL
		1	Commander, Watervliet Arsenal, Watervliet, NY 12189
		1	ATTN: Dr. T. Davidson

No. of Copies	To
1	Cummins Engine Company, Columbus, IN 47201 ATTN: Mr. R. Kamo
1	Defence Research Establishment Pacific, FMO, Victoria, B.C., VOS 1B0, Canada ATTN: R. D. Barer
1	Deposits and Composites, Inc., 1821 Michael Faraday Drive, Reston, VA 22090 ATTN: Mr. R. E. Engdahl
1	Electric Power Research Institute, P.O. Box 10412, 3412 Hillview Avenue, Palo Alto, CA 94304 ATTN: Dr. A. Cohn
1	European Research Office, 223 Old Maryleborne Road, London, NW1 - 5the, England ATTN: Dr. R. Quattrone LT COL James Kennedy
1	Ford Motor Company, Turbine Research Department, 20000 Rotunda Drive, Dearborn, MI 48121 ATTN: Mr. A. F. McLean Mr. E. A. Fisher Mr. J. A. Mangels Dr. R. Govila
1	General Atomic Company, P.O. Box 81608, San Diego, CA 92138 ATTN: Jim Halzgraf
1	General Electric Company, Mail Drop H-99, Cincinnati, OH 45215 ATTN: Mr. Warren Nelson
1	General Electric Company, Research and Develop- ment Center, Box 8, Schenectady, NY 12345 ATTN: Dr. R. J. Charles Dr. C. D. Greskovich Dr. S. Prochazka
1	General Motors Corporation, AC Spark Plug Division, Flint, MI 48556 ATTN: Mr. Fred Kennard
1	Georgia Institute of Technology, EES, Atlanta, GA 30332 ATTN: Mr. J. D. Walton
1	GTE Laboratories, Waltham Reserach Center, 40 Sylvan Road, Waltham, MA 02154 ATTN: Dr. C. Quackenbush Dr. W. H. Rhodes
1	IIT Research Institute, 10 West 35th Street, Chicago, IL 60616 ATTN: Mr. S. Bortz, Director, Ceramics Division Dr. D. Larsen
1	Institut fur Werkstoff-Forschung, DFVLR, 505 Porz-Wahn, Linder Hohe, Germany ATTN: Dr. W. Bunk
1	Institut fur Werkstoff-Forschung, DFVLR, 5000 Koln 90(Porz), Linder Hohe, Germany ATTN: Dr. Ing Jurgen Heinrich
1	International Harvester, Solar Division, 2200 Pacific Highway, P.O. Box 80966, San Diego, CA 92138 ATTN: Dr. A. Metcalfe Ms. M. E. Gulden

No. of Copies	To
1	Jet Propulsion Laboratory, C.I.T., 4800 Oak Grove Drive, Pasadena, CA 91103 ATTN: Dr. Richard Smoak
1	Mr. Edward Kraft, Product Development Manager, Industrial Sales Division, Kyocera International, Inc., 8611 Balboa Avenue, San Diego, CA 92123
1	Martin Marietta Laboratories, 1450 South Rolling Road, Baltimore, MD 21227 ATTN: Dr. J. Venables
1	Massachusetts Institute of Technology, Department of Metallurgy and Materials Science, Cambridge, MA 02139 ATTN: Prof. R. L. Coble Prof. H. K. Bowen Prof. W. D. Kingery Prof. D. Clarke
1	Materials Research Laboratories, P.O. Box 50, Ascot Vale, VIC 3032, Australia ATTN: Dr. C. W. Weaver
1	Midwest Research Institute, 425 Volker Boulevard, Kansas City, MO 64110 ATTN: Mr. Gordon W. Gross, Head, Physics Station
1	Dr. Howard Mizuhara, GTE-Wesgo, 477 Harbor Boulevard, Belmont, CA 94002
1	Norton Company, Worcester, MA 01606 ATTN: Dr. N. Ault Dr. M. L. Torti
1	Pennsylvania State University, Materials Research Laboratory, Materials Science Department, University Park, PA 16802 ATTN: Prof. R. Roy Prof. R. E. Newnham Prof. R. E. Tressler Prof. R. Bradt Prof. V. S. Stubican
1	Pratt and Whitney Aircraft, P.O. Box 2691, West Palm Beach, FL 33402 ATTN: Mr. Mel Mendelson
1	PSC, Box 1044, APO San Francisco 96328 ATTN: MAJ A. Anthony Borges
1	RIAS, Division of the Martin Company, Baltimore, MD 21203 ATTN: Dr. A. R. C. Westwood
1	Rockwell International Science Center, 1049 Camino Dos Rios, Thousand Oaks, CA 91360 ATTN: Dr. F. Lange
1	Royal Aircraft Establishment, Materials Depart- ment, R 178 Building, Farnborough, Hants, England ATTN: Dr. N. Corney
1	Shane Associates, Inc., 7821 Carrleigh Parkway, Springfield, VA 22152 ATTN: Dr. Robert S. Shane, Consultant
1	Silag Inc., P.O. Drawer H, Old Buncombe at Poplar Greer, SC 29651 ATTN: Dr. Bryant C. Bechtold

No. of Copies	To
1	Director, Eustis Directorate, U.S. Army Mobility Research and Development Laboratory, Fort Eustis, VA 23604 ATTN: Mr. J. Robinson, DAVDL-E-MOS (AVRADCOM)
1	Mr. C. Walker
1	Chief of Naval Research, Arlington, VA 22217 ATTN: Code 471
1	Dr. A. Diness
1	Dr. R. Pohanka
1	Naval Research Laboratory, Washington, DC 20375 ATTN: Dr. J. M. Krafft - Code 5830
1	Mr. R. Rice
1	Dr. D. Lewis
1	Dr. Jim C. I. Chang
1	Headquarters, Naval Air Systems Command, Washington, DC 20360 ATTN: Code 5203
1	Code MAT-042M
1	Headquarters, Naval Sea Systems Command, 1941 Jefferson Davis Highway, Arlington, VA 22376 ATTN: Code 035
1	Commander, Naval Material Industrial Resources Office, Building 537-2, Philadelphia Naval Base, Philadelphia, PA 19112 ATTN: Technical Director
1	Commander, Naval Weapons Center, China Lake, CA 93555 ATTN: Mr. F. Markarian
1	Mr. E. Teppo
1	Mr. M. Ritchie
1	Commander, U.S. Air Force of Scientific Research, Building 410, Bolling Air Force Base, Washington, DC 20332 ATTN: MAJ W. Simmons
1	Commander, U.S. Air Force Wright Aeronautical Laboratories, Wright-Patterson Air Force Base, OH 45433 ATTN: AFWAL/MLLM, Dr. N. Tallan
1	AFWAL/MLLM, Dr. H. Graham
1	AFWAL/MLLM, Dr. R. Ruh
1	AFWAL/MLLM, Dr. A. Katz
1	AFWAL/MLLM, Mr. K. S. Mazdidasni
1	Aero Propulsion Labs, Mr. R. March
1	National Aeronautics and Space Administration, Washington, DC 20546 ATTN: Mr. G. C. Deutsch - Code RW
1	Mr. J. Gangler
1	AFSS-AD, Office of Scientific and Technical Information
1	National Aeronautics and Space Administration, Lewis Research Center, 21000 Brookpark Road, Cleveland, OH 44135 ATTN: J. Accurio, USAMRDL
1	Dr. H. B. Probst, MS 49-1
1	Dr. R. Ashbrook
1	Dr. S. Dutta
1	Mr. S. Grisaffe

No. of Copies	To
1	National Aeronautics and Space Administration, Langley Research Center, Hampton, VA 23665 ATTN: Mr. J. Buckley, Mail Stop 387
1	Department of Energy, Division of Transportation, 20 Massachusetts Avenue, N.W., Washington, DC 20545 ATTN: Mr. George Thur (TEC)
1	Mr. Robert Schulz (TEC)
1	Mr. John Neal (CLNRT)
1	Mr. Steve Wander (Fossil Fuels)
1	Mechanical Properties Data Center, Belfour Stulen Inc., 13917 W. Bay Shore Drive, Traverse City, MI 49684
1	National Bureau of Standards, Washington, DC 20234 ATTN: Dr. S. Wiederhorn
1	Dr. J. B. Wachtman
1	Dr. S. Freiman
1	National Research Council, National Materials Advisory Board, 2101 Constitution Avenue, Washington, DC 20418 ATTN: D. Groves
1	R. M. Spriggs
1	National Science Foundation, Washington, DC 20550 ATTN: B. A. Wilcox
1	Admiralty Materials Technology Establishment, Polle, Dorset BH16 6JU, UK ATTN: Dr. D. Godfrey
1	Dr. M. Lindley
1	AiResearch Manufacturing Company, AiResearch Casting Company, 2525 West 190th Street, Torrance, CA 90505 ATTN: Mr. K. Styhr
1	Dr. D. Kotchief
1	AiResearch Manufacturing Company, Materials Engineering Dept., 111 South 34th Street, P.O. Box 5217, Phoenix, AZ 85010 ATTN: Dr. D. W. Richerson, MS 93-393/503-44
1	Dr. J. Smyth
1	AVCO Corporation, Applied Technology Division, Lowell Industrial Park, Lowell, MA 01887 ATTN: Dr. T. Vasilos
1	Carborundum Company, Research and Development Division, P.O. Box 1054, Niagara Falls, NY 14302 ATTN: Dr. J. A. Coppola
1	Dr. M. Srinivasan
1	Case Western Reserve University, Department of Metallurgy, Cleveland, OH 44106 ATTN: Prof. A. H. Heuer
1	Ceradyne, Inc., P.O. Box 11030, 3030 South Red Hill Avenue, Santa Ana, CA 92705 ATTN: Dr. Richard Palicka
1	Combustion Engineering, Inc., 911 West Main Street, Chattanooga, TN 37402 ATTN: C. H. Sump

No. of Copies	To
1	Solar Turbine International, 2200 Pacific Coast Highway, San Diego, CA 92138 ATTN: Mr. Andrew Russe1, Mail Zone R-1
1	Stanford Research International, 333 Ravenswood Avenue, Menlo Park, CA 94025 ATTN: Dr. P. Jorgensen
1	Dr. D. Rowcliffe
1	State University of New York at Stony Brook, Department of Materials Science, Long Island, NY 11790 ATTN: Prof. Franklin F. Y. Wang
1	TRW Defense and Space Systems Group, Redondo Beach, CA 90278 ATTN: Francis E. Fendell
1	United Technologies Research Center, East Hartford, CT 06108 ATTN: Dr. J. Brennan
1	Dr. F. Galasso
1	University of California, Lawrence Livermore Laboratory, P.O. Box 808, Livermore, CA 94550 ATTN: Mr. R. Landingham
1	Dr. C. F. Cline
1	University of Florida, Department of Materials Science and Engineering, Gainesville, FL 32601 ATTN: Dr. L. Hench
1	University of Massachusetts, Department of Mechanical Engineering, Amherst, MA 01003 ATTN: Prof. K. Jakus
1	Prof. J. Ritter

No. of Copies	To
1	University of Newcastle Upon Tyne, Department of Metallurgy and Engineering Materials, Newcastle Upon Tyne, NE1 7 RU, England ATTN: Prof. K. H. Jack
1	University of Washington, Ceramic Engineering Division, FB-10, Seattle, WA 98195 ATTN: Prof. James I. Mueller
1	Virginia Polytechnic Institute, Department of Materials Engineering, Blacksburg, VA 24061 Prof. D. P. H. Hasseiman
1	Westinghouse Electric Corporation, Research Laboratories, Pittsburgh, PA 15235 ATTN: Dr. R. J. Bratton
1	Dr. B. Rossing
1	Mr. Joseph T. Bailey, 3M Company, Technical Ceramic Products Division, 3M Center, Building 207-1W, St. Paul, MN 55101
1	Dr. Jacob Stiglich, Dart Industries/San Fernando Laboratories, 10258 Norris Avenue, Pacoima, CA 91331
1	Dr. J. Petrovic - CMB-5, Mail Stop 730, Los Alamos Scientific Laboratories, Los Alamos, NM 87545
1	Mr. R. J. Zentner, EAI Corporation, 198 Thomas Johnson Drive, Suite 16, Frederick, MD 21701
2	Director, Army Materials and Mechanics Research Center, Watertown, MA 02172 ATTN: DRXMR-PL

END

DATE
FILMED

9 83

DT